Scale model tests of a 170-meter high sculptural tower

Autor(en): **Umemura, Hajime / Tada, Hideyuki / Sonobe, Yasuhisa**

Objekttyp: **Article**

Zeitschrift: **IABSE congress report = Rapport du congrès AIPC = IVBH Kongressbericht**

Band (Jahr): **9 (1972)**

PDF erstellt am: **21.07.2024**

Persistenter Link: https://doi.org/10.5169/seals-9611

V

Scale Model Tests of a 170-meter High Sculptural Tower

Essais sur modèle réduit d'une tour de 170 m de hauteur

Versuche am massstäblichen Modell eines Turmbauwerkes von 170 m Höhe

HAJIME UMEMURA
Professor at the University of Tokyo, Eng.D., Japan

HIDEYUKI TADA
Associate Director, Nikken Sekkei Ltd, Eng.D., Japan

YASUHISA SONOBE
Professor at Chiba Institute of Technology, Eng.D., Japan

1. Introduction

The 170 m high PL Peace Tower, shown in Figs. 1 and 2, was constructed in Osaka, Japan in 1970. The tower is composed of a rigid reinforced concrete foundation which supports a 12 m high steel framed reinforced concrete podium of rigid construction which in turn supports a tubular steel tower structure. The tower portion is covered with a shotcreted crust which makes the tower into a huge sculpture of highly complicated configuration. In order to obtain basic data for earthquake and wind resistant design of this tower of unprecedented shape, extensive research studies comprising observation of micro tremors of the ground; wind tunnel tests using 1/100 scale models; static loading tests on 1/33 models including those tested to failure; free vibration tests; bending and shearing tests on shotcreted crust of the tower models, etc. were conducted. In addition, the actual vibration of the tower was observed upon its completion.

Fig. 1 PL Peace Tower

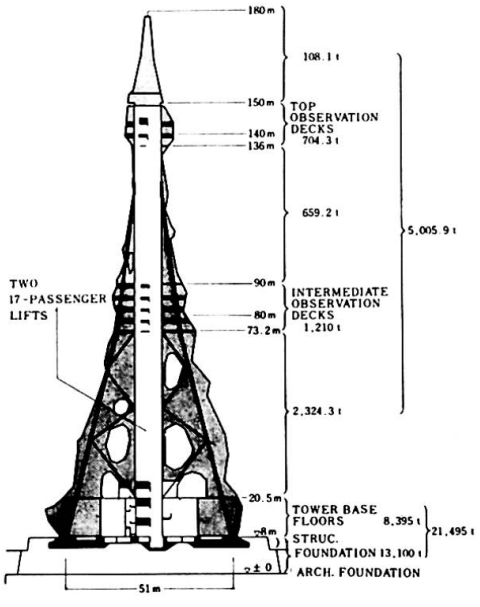

Fig.2 Illustrative Drawing

This report deals with the experimental test on 1/33 scale models conducted for the purpose of obtaining some basic data on which to base a simulated vibration model for a dynamic structural analysis. The experiments consisted of the load-by-gravity tests, the concentrated lateral load tests and the free vibration tests at various loading stages. While the load-by-gravity tests were non-rupture tests in which the lateral forces proportional to the weights of various parts of the tower were applied, the concentrated lateral loading tests were carried to the failure of the specimens.

2. Test Models

Based on the original design height of the tower which was 160 m, the scale of 1/33 was adopted for the models, taking into account the available space of the testing station. This scale resulted in the models having a height of 4.697 m, with all other dimensions similarly reduced, the original form of the proposed tower being maintained. The models were framed by the use of the same materials as those used for the actual tower, i.e., [] - 150 x 75 x 20 x 4.5 for the central shaft and steel bars for inclined columns, diagonal webs and upper framework of the tower. Two models, A and B, were prepared, both provided with horizontal diaphragms so as to facilitate the preparation of the tower shaft which was of a very complicated form. The models were designed to have sectional area of steel five times as large as that proportional to a 1/33 scale model.

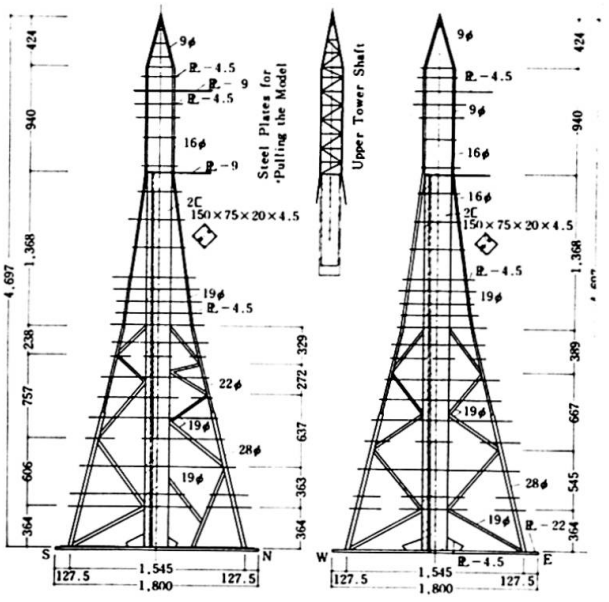

Fig. 3 Framing of the Model

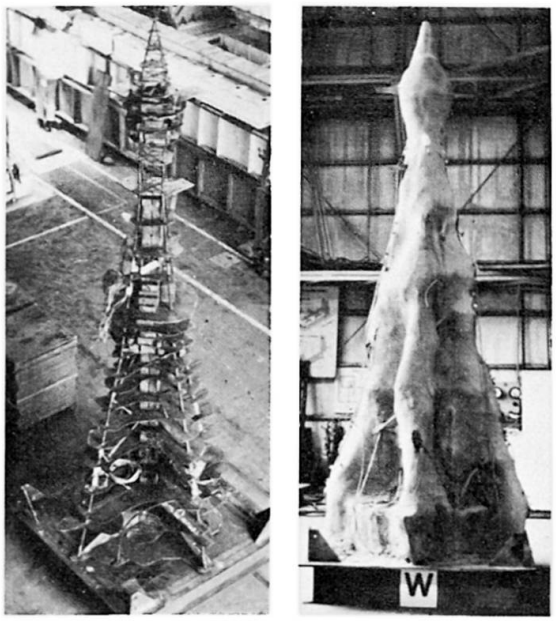

Fig. 4 Model

The outer crusts of these models were composed of shotcrete on wire laths placed on the outer face of diaphragms, all applied in the same manner as proposed for the actual tower.

The models were somewhat simplified when compared with the actual tower which, with self-standing columns and branch-like members, is very complicated; however, the basic characteristics of the tower configuration is considered fairly well represented by the models. The cross sectional area of the shotcrete crust turned out to be 11 times and 14.5 times as large as that proportional to 1/33 models with regard to Model A and Model B respectively.
In the load-by-gravity tests where the test loads were casued by the models' own weight, slabs of steel were attached to the upper and intermediate observation deck levels so as to cause the gravity loads corresponding to the loads to which these decks would be subjected to.

Tables 1 and 2 show the measured data of the completed models. Mechanical properties of shotcreted crust and structural steel are shown in Tables 3 and 4. The load-by-gravity tests and concentrated load tests were conducted when the shotcrete was aged one week and five weeks respectively.

Table 1. Weight of Models

	Model A	Model B
	(kg)	(kg)
Steel frame, Diaphragm	690	690
Added weight	500	500
Total steel weight	1 190	1 190
Shotcrete (ρ = specific gravity)	570 (ρ = 2.01)	570 (ρ = 2.14)
Total weight	1 760	1 990
Mean thickness of shotcrete	2.18 cm	2.89 cm

Table 3. Mechanical Properties of Steel

Steel	Sectional area	Yield point	Tensile strength	Elongation ratio
	(cm^2)	(t/cm^2)	(t/cm^2)	(%)
28 ø	6.256	2.86	4.47	32
22 ø	3.841	3.04	4.98	30
19 ø	2.821	3.07	4.93	31
16 ø	2.019	2.96	4.56	33
9 ø	0.593	2.86	4.29	33
℄- 4.5 ([]- 150 x 75 x 20 x 4.5)	-	2.73	4.04	32

Table 2. Relationship of Cross Section and Weight of Actual Structure to Those of Models

		Values by measurement on models	Values as designed for models
Model A	Sectional area of steel	$(\ )^2 \times 5$	$(\ )^2 \times 5$
	Sectional area of shotcrete	$(\ )^2 \times 11$	$(\ )^2 \times 5$
	Total weight	$(\ )^3 \times 17.6$	$(\ )^3 \times 10$
Model B	Sectional area of steel	$(\ )^2 \times 5$	$(\ )^2 \times 5$
	Sectional area of shotcrete	$(\ )^2 \times 14.5$	$(\ )^2 \times 5$
	Total weight	$(\ )^3 \times 20$	$(\ )^3 \times 10$

( ) = Value proportional to 1/33 scale model

Table 4. Mechanical Properties of Shotcrete

	Material age	Compressive strength (kg/cm^2)	Crushing strength (kg/cm^2)	Young's Modulus ($\times 10^5$ kg/cm^2)
Model A	1 week	298	28.7	1.97
	5 weeks	386	-	1.82
Model B	1 week	174	16.0	1.43
	5 weeks	165	-	1.20

3. Methods of Testing

Of the two loading methods, the loading-by-gravity was planned so that the lateral loads proportional to various members would be imposed on the members. For this purpose, the models were fixed at the base and were turned up and down. This type of loading may be considered to have simulated the conditions caused by the vibration of the fundamental mode. The intensity of the loading was rather small compared with the strength of materials used for the models; therefore, the experiments were conducted only within the elastic range of the models. On the contrary, the concentrated loading was intended to simulate the conditions under the ultimate loading.

In the load-by-gravity tests, each model constructed in an upright position was placed on a rotating hub of the testing apparatus together with the tower-shaped gauge holders which surrounded the model and the model was turned up and down 180° as shown in Figs. 5 and 6. In turning round the model the angle of rotation was controlled by means of a chain block and a pulley. The rotation was in north-south direction. The deflections of the models were measured with dial gauges whereas their strain were measured with wire strain gauges. The behaviours of steel under loading were observed by means of high-sensitive semi-conductor gauges which were used in combination with the aforesaid gauges. In addition, a total of nine measurement instruments as shown in Fig.7, four on compressive side and five on tensile side, were mounted along the outermost faces of each model in order to measure the local curvature variation of the outer crust.

For the concentrated loading tests, the model was connected to the loading wall by the use of a cable, which was pulled by means of a chain block so that a tensile force was imposed on the model. The cable was so supported as to be in a horizontal position during the test. For each model, the deflection was measured at Point 1 (apex), Point 2 (4.048 m in height) and Point 3 (3.333 m in height), and the load was imposed at Points 2 and 3. Deflections and strains were measured by the use of same instruments as those used for the load-by-gravity tests.

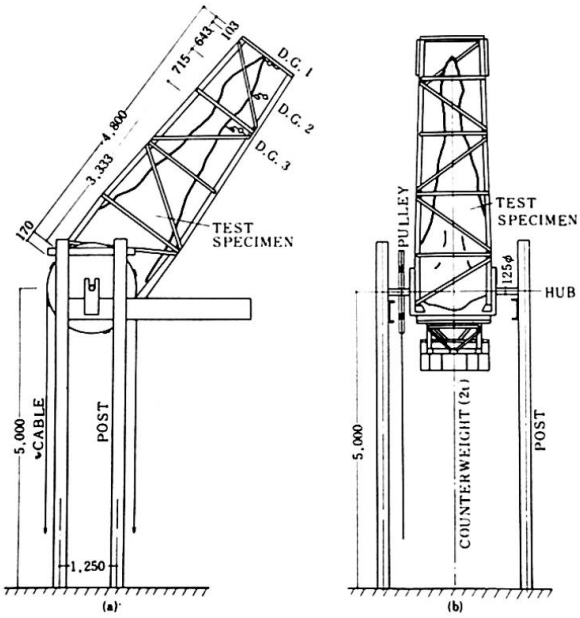

Fig. 5 Loading Apparatus

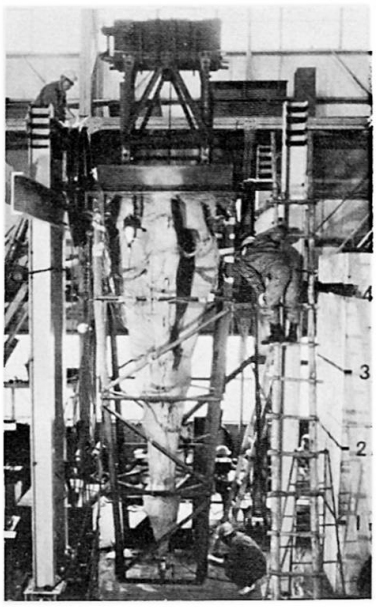

Fig. 6

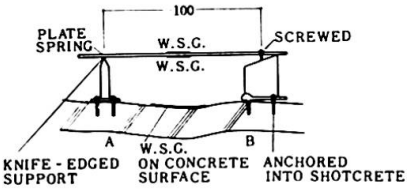

Fig. 7 Curvature Measurement Instrument

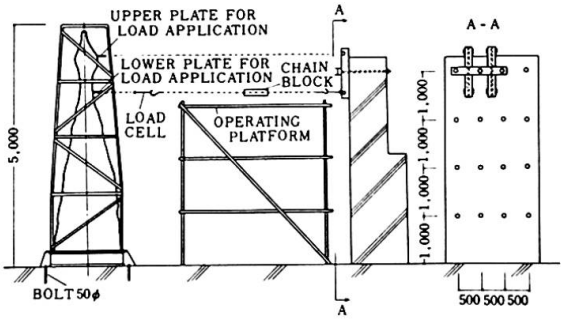

Fig. 8 Concentrated Loading Apparatus

4. Test Results

No cracks whatsoever were caused to the models by the load-by-gravity tests. Fig. 9 shows the load-deflection curves for these tests. It was generally found that the force normal to the axis of the tower (expressed $K = \sin\theta$, where θ = rotation angle) and the deflection were in a linear relationship; however, some decrease of rigidity was observed when the rotation angle approached $\theta = \pi/2$. Table 5 shows the results of studies on the initial rigidity values as observed at Points 1, 2 and 3 during the tests. In the table, the theoretical rigidity values for the case where the model was assumed to be a solid cantilever having the moments of inertia equal to those of the various horizontal sectional areas were taken as 1. Further, the theoretical values for the case where steel frame alone was considered effective are shown in Column 1 and the foregoing values modified by considering the curvature variation of the outer crust as will be discussed later are shown in Column 2 of the table. Column 3 of the same table shows the measured rigidity values.

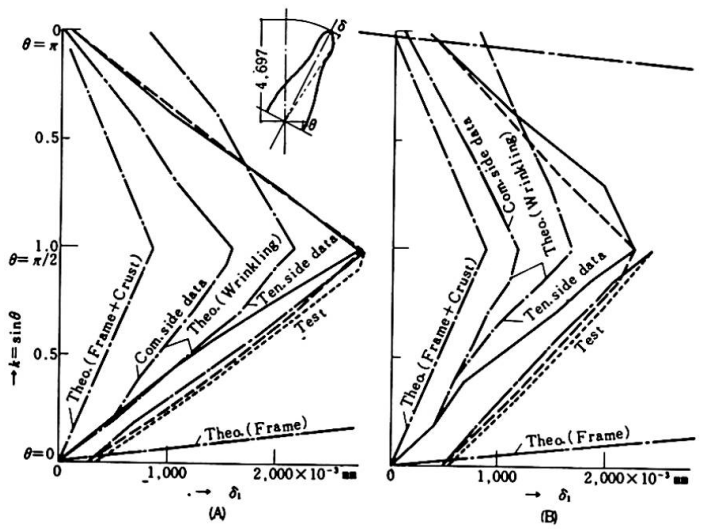

Fig. 9 Load-Deflection Curve

Table 5. Rigidity Ratio

The rigidity of the solid cantilever as described in Para. 5 being taken as unity.

		Model A			Model B		
	Measuring points	1	2	3	1	2	3
1	Rigidity ratio where steel frame only is effective	0.057	0.089	0.123	0.049	0.058	0.096
2	Rigidity ratio where the local bending of crust is taken into account in analysis	0.47	0.47	0.40	0.64	0.64	0.63
3	Rigidity ratio based on initial values obtained by tests	0.34	0.33	0.33	0.46	0.47	0.50

If the theoretical rigidity value of the solid cantilever was taken as 100%, the measured values for Model A and Model B were 33% and 50% respectively. It is believed that the initial rigidities as observed during the experiments are fairly well accounted for by the modified values shown in Column 2 of the table. The deformations at the apex of the models were 2.40 mm for Model A and 2.14 mm for Model B.

Fig. 10 shows the load-deflection curves; Table 6, the initial rigidity ratios of models; and Table 7, yield strength, ultimate strength and corresponding deformations; all for concentrated loading tests.

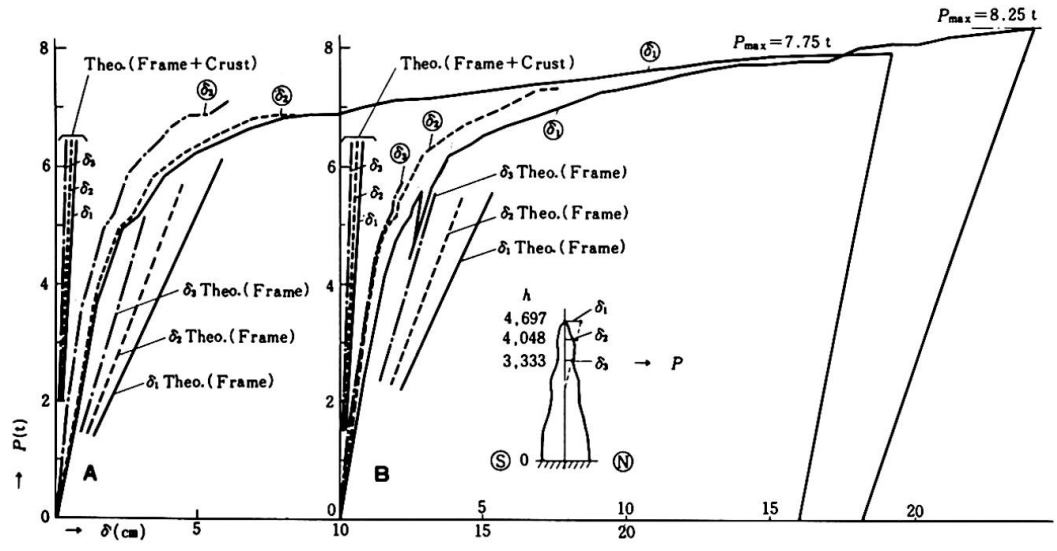

Fig. 10 Load-Deflection Curve

Table 6. Rigidity Ratio

The rigidity of the solid cantilever as described in Para.5 being taken as unity.

		Model A				Model B			
Measuring points		1	2	3	Mean	1	2	3	Mean
Initial rigidity by tests	Loading or upper part	0.23	0.19	0.30	0.24	0.27	0.30	0.34	0.30
Rigidity	Loading on lower part	0.32	0.31	0.29	0.31	0.56	0.21	0.44	0.40

Table 7. Permissible Load Bearing Capacity Proved by Tests

	Points of Load Application	Permissible load (R = 1/200)		Permissible load (R = 1/100)		Permissible load (Max)	
		Py(t)	δ top (cm)	Py'(t)	δ top (cm)	P max(t)	δ top (cm)
Model A	Upper part	1.5	2.5	2.08	5.0	2.17	6.1 (1/79)
	Lower part	5.0	2.5	6.2	5.0	7.75	30 (1/16)
Model B	Upper part	1.86	2.5	-	-	2.68	4.8 (1/100)
	Lower part	5.15	2.5	6.5	5.0	8.25	24 (1/20)

Values in ( ) represent joint translation angles.

Table 8. Permissible Load Bearing Capacity Proved by Analysis
(up to Level 1.965 m)

	Yield point of column / Yield point of shaft	Yield point of column / Strength of shaft	Strength of column / Yield point of shaft	Strength of column / Strength of shaft
Permissible Load	5.82 t (A 0.75) (B 0.71)	6.75 t (A 0.87) (B 0.82)	8.15 t (A 1.05) (B 0.99)	9.10 t

Values in ( ) represent $\frac{\text{Value resulting from analysis}}{\text{Theoretical value}}$

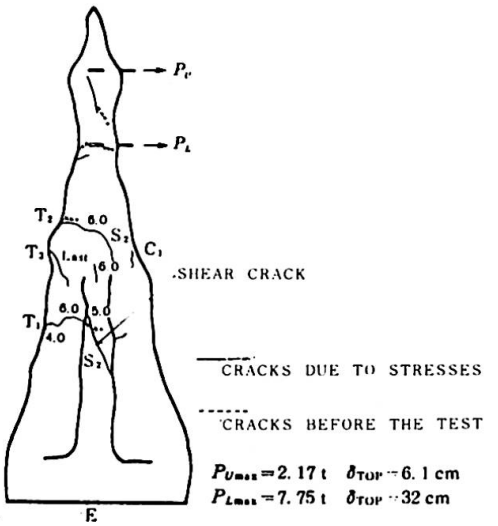

Fig. 11 Cracks Caused by the Concentrated Loading Test

A few examples are indicated in Fig. 11 to show how cracks appeared in the shotcreted crusts of the models. Some cracks had already took place prior to the tests because of the shrinkage due to drying. The cracks due to stresses in shotcrete were first caused by the shrinkage on the tensile side. They were followed by the vertical cracks and crushing on the compressive side at the next stage, and by the shear cracks at the ultimate stage.

Where the load was applied to the upper part of the model, the strength was governed by the shear resistance of the shotcrete at the point of load application. Where the load was applied to the lower part, the buckling of the steel column in compression located between the diaphragms was the governing factor. The different structural behaviours under the loads applied to different points of models resulted in the difference in permissible strengths shown in Table 7. In Table 8, the sums of the load bearing capacity of steel columns and that of central shaft, both as obtained by the analysis for the case where the load was applied to the lower part of the model, are compared with the corresponding load bearing capacity as obtained by the tests. The bearing capacity referred to above was taken as being equal to the yield point or strength of the material. For the central shaft, however, a certain elasto-plastic coefficient was assumed, and the bearing capacity contributed by the columns was computed on the assumption that the lever arm was equal to the spacing of the columns. It may be induced from the table that the steel members partially entered a state of strain hardening, and the shotcreted elements also contributed to increase the bearing capacity on the compressive side.

5. Deformation of Shotcrete Crust and Its Effects on Tower Structure Deflection

Fig. 12 indicates the relationship between the loads and the curvature variations due to stresses in shotcreted elements.

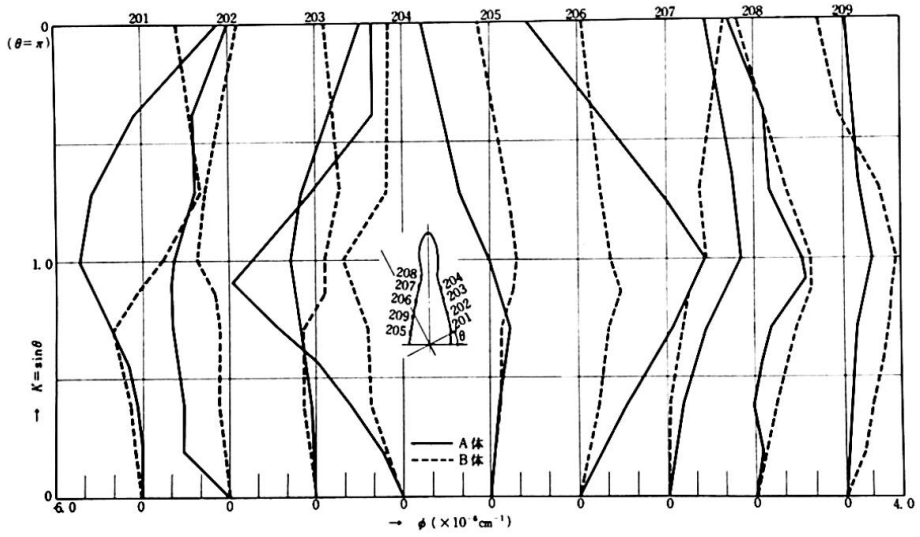

Fig. 12 Load-Curvature Curve

It is assumed that the overall deflection of the tower is a summation of (1) and (2) described below:

(1) Deflection of an imaginary solid cantilever beam in which shotcreted crust is fully integrated with steel frame. The solid cantilever beam is assumed to have the moments of inertia equal to those of the various cross sections involved.

(2) Deflection caused by the local bending of the shotcrete crust located on compressive and tensile extreme fibres of the tower structure. Because of the surface irregularities along the generating line of the tower shaft, this type of deflection was taken into account.

For Type (2) deflection, the analyses have been made as follows:
The part (approx. 10 cm in length) for which the curvature due to stresses in shotcrete crust was measured was assumed to form an arc-shaped section. If

the length of this arc, the length of the corresponding chord and the curvature after deformation are expressed as ℓ , χ and ϕ (where ϕ = the original curvature ϕ_0 + the curvature variation due to stresses $\Delta\phi$) respectively, then,

$$\chi = 2\frac{\sin(\frac{\ell}{2}\cdot\phi)}{\phi} \quad \cdots\cdots (5.1)$$

If it is further assumed that the change of ℓ does not give any influence on the deflection caused by the bending of shotcreted elements described in (2), then ℓ may be considered constant in Equation (5.1). From this equation, the variations of chord length χ can be obtained in proportion to the measured curvature variations $\Delta\phi$ caused by the stresses in rigid shotcreted elements. By adopting the expression that,

$$X = \chi/\chi_0 \ , \quad \Phi = \phi/\phi_0$$

(where χ_0 and ϕ_0 represent the chord length and curvature prior to deformation.)
the following equation can be written:

$$X = \frac{\sin(\frac{\ell}{2}\phi_0\Phi)}{\Phi\sin(\frac{\ell}{2}\phi_0)} \quad \cdots\cdots (5.2)$$

The increase of X expressed as $\Delta X (=\Delta\chi/\chi_0)$ resulting from the increase of Φ expressed as $\Delta\Phi (=\Delta\phi/\phi_0)$ can then be written as follows provided that $\Delta\Phi$ is very small:

$$\Delta X = \left(\frac{dX}{d\Phi}\right)_{\Phi=1}\cdot\Delta\Phi$$

$$\therefore \Delta X = \left(\frac{\ell}{2}\phi_0\cot\frac{\ell}{2}\phi_0 - 1\right)\cdot\Delta\Phi \quad \cdots\cdots (5.3)$$

And from the measurement results, we have,

$$|\Delta\Phi| \leq 0.046 \quad \cdots\cdots (5.4)$$

It should be noted that ΔX in Equation (5.3) corresponds to the strains at the tensile and compressive extreme fibres with regard to the plane perpendicular to the axis of the tower. The ΔX referred to above, however, was modified by multiplying it by the cosine corresponding to the axis of the tower at the points where measurement was taken.

The values of curvature for the tower as a whole were obtained by linear interpolation for the part in between the measuring points whereas the values obtained at the nearest measuring points were adopted without modification for the apex and base outside the measuring points.

The results of analyses so far described are plotted on Fig. 9 and Table 5. In case of Model A, the load-deflection curves as obtained from the analyses, the theoretical curves in which $\theta = 0 \sim \pi/16$ and coefficient of seismic force $k = 0 - 0.2$ coincide well with the measured curves until the coefficient k reaches 0.5 approximately at which value the measured curves begin to show the decrease of rigidity. In case of Model B, the curves for theoretical values coincide well with those for measured values until the seismic coefficient reaches 0.4 or so where the rigidity begins to decrease as can be observed from the curves for measured values. Unlike Model A, it is noticed in Model B that the theoretical curves show smaller deflections than measured curves for the same coefficient. The values shown at the column 3 of Table 5 are the arithmetical means of the theoretical values computed for the compressive side and those computed for the tensile side, both at the point where $k = 1.0$ and $\theta = \pi/2$.

6. Reflection of Test Results on the Design

A micro-vibration test conducted with a pick-up placed at Measurement Point 2 indicated the primary natural period of T_1 = 0.080 sec and the damping constant of h = 2% for Model A. The corresponding values for Model B were T_1 = 0.079 sec and h = 2.8%, as shown in Table 9.

Table 9. Vibration Test Results
(at Measuring Point 2)

		Before load application	After the upper part was loaded to failure of the model	After the lower part was loaded to failure of the model
Model A	T_1	0.080 sec	0.083 sec	0.092 sec
	h	2.0 %	2.3 %	0.64 %
Model B	T_1	0.079 sec	0.084 sec	0.103 sec
	h	2.8 %	1.8 %	0.68 %

T_1 : fundamental period (sec) h : damping coefficient (%)
Pick up period = 1 sec

In the load-by-gravity tests where the maximum deflection at the apex was y cm, the values of c at T = $\sqrt{y}$ /c were 6.1 and 5.9 for Model A and Model B respectively. When the theoretical value T_1 = 0.95 sec as computed on the assumption that the tower was a solid cantilever beam was compensated by a factor for initial rigidity decrease, then T_1 = 1.66 sec and T_1 = 1.40 sec were obtained for Model A and Model B respectively.

As it became possible to predict the characteristics of vibration and the mechanism of rupture of the actual tower, the natural period and damping coefficient were assumed by reference to the values obtained by the experiment, and the tower's response to various pattern of earthquake waves was computed for analysis to provide the data on which to base the cross sections at the final design stage. As for the effects of external forces, earthquakes rather than wind loads were found to give greater influence, and consequently seismic resistance became the primary design consideration. The measured periods of actual tower under the influence of micro-tremors were found to be 1.82 sec (h = 0.6%) for the fundamental mode of vibration. The similar values for the secondary and the tertiary modes were 0.6 sec and 0.31 respectively.

7. Conclusions

The major findings observed in the experiments using 1/33 scale models may be summarized as follows:

(1) Despite an unprecedented testing method employed for the load-by-gravity tests, the experiment was carried out without encountering much difficulty.

(2) The rigidity of the models subjected to the load-by-gravity tests was found to have the values intermediate between the rigidity of the structure in which shotcreted crust and steel frame are considered fully integrated to form effective sectional area and the rigidity of structure for which steel frame only forms effective sectional area. The measured rigidity of Model A was approximately 1/3 of the value which would have been obtained if the entire combined sections had been effective. This relative value was about 1/2 in case of Model B which had a thicker crust. A similar tendency was observed during the concentrated tests from which it was found that the values of initial rigidity were about 1/4 - 1/3 and about 1/3 - 1/2 for Model A and Model B respectively. The rigidity values thus made predictable from the experiments were considered reasonably accurate to serve the

purpose of the structural design which ensued.

(3) In the concentrated loading tests, the load-bearing capacity of the model loaded at the upper part was governed by the shear resistance of the shotcrete at the point to which the load was applied whereas the capacity was governed by the buckling of the steel in compression in case the load was applied to the lower part. The deflection of the apexes of the models reached 1/16 - 1/20 in these cases, which was considered indicative of sufficient ductility.

(4) The natural periods of the models tended to prolong as the fracture progressed. This tendency was considered due to the decrease of rigidity. On the contrary, the damping constant tended to decrease as the fracture progressed.

(5) When the rigidity of shotcrete was taken into account based on technological evaluation of the test results in order to simulate vibration models for analysis, the fundamental period and damping constant became 1.84 and 2% respectively.

(6) The tower was constructed to the design which was based on the results of these experiments. The natural period of the actual tower under micro tremors was observed and found to coincide well with that of the models.

Summary

In order to obtain the data for earthquake-resistant design of a 170 m high sculptural tower composed of steel frames and shotcreted crust, loading tests were conducted on 1/33 scale models. For the loading tests, the models were fixed at the base and turned up and down. Thus, the members involved were subjected to lateral forces proportional to their weight nearly in the same way as they would be under earthquakes. It was indicated by these experiments that the rigidity of models could be accounted for by taking into consideration the local bending of shotcrete. The tests also helped to clarify the structural behaviours under ultimate loads. The experiments served their intended purposes satisfactorily as the test results were in many ways reflected in the final design.

Bibliography

Research study on the seismic resistance of PL Peace Tower, by H. Tada and Y. Sonobe, Synopses of Transactions, Architectural Institute of Japan, November 1971.

PL Peace Tower, edited by Nikken Sekkei Ltd, Geijutsu Seikatsu Sha, August 1970.